

Bathroom greywater recycling using polyelectrolyte-complex bilayer membrane: Advanced study of membrane structure and treatment efficiency



K.S. Oh^a, P.E. Poh^{a,b,*}, M.N. Chong^{a,b}, E.S. Chan^a, E.V. Lau^c, C.P. Saint^d

^a Chemical Engineering Discipline, School of Engineering, Monash University Malaysia Campus, Jalan Lagoon Selatan, 47500 Bandar Sunway, Selangor, Malaysia

^b Sustainable Water Alliance, Advanced Engineering Platform, Monash University Malaysia Campus, Jalan Lagoon Selatan, 47500 Bandar Sunway, Selangor, Malaysia

^c Mechanical Engineering Discipline, School of Engineering, Monash University Malaysia Campus, Jalan Lagoon Selatan, 47500 Bandar Sunway, Selangor DE, Malaysia

^d Natural & Built Environments Research Centre, University of South Australia, Mawson Lakes Campus, Mawson Lakes, 5095 South Australia, Australia

ARTICLE INFO

Article history:

Received 28 January 2016

Received in revised form 31 March 2016

Accepted 9 April 2016

Available online 13 April 2016

Keywords:

Chitosan
Alginate
Bilayer membrane
Molecular cut-off
Greywater
Filtration

ABSTRACT

Polyelectrolyte-complex bilayer membrane (PCBM) was fabricated using biodegradable chitosan and alginate polymers for subsequent application in the treatment of bathroom greywater. In this study, the properties of PCBM were studied and it was found that the formation of polyelectrolyte network reduced the molecular weight cut-off (MWCO) from 242 kDa in chitosan membrane to 2.71 kDa in PCBM. The decrease in MWCO of PCBM results in better greywater treatment efficiency, subsequently demonstrated in a greywater filtration study where treated greywater effluent met the household reclaimed water standard of <2 NTU turbidity and <30 ppm total suspended solids (TSS). In addition, a further 20% improvement in chemical oxygen demand (COD) removal was achieved as compared to a single layer chitosan membrane. Results from this study show that the biodegradable PCBM is a potential membrane material in producing clean treated greywater for non-potable applications.

© 2016 Elsevier Ltd. All rights reserved.

1. Introduction

Chitosan (*D*-glucosamine and *N*-acetyl-*D*-glucosamine) is a polycationic biopolymer extracted from the exoskeleton of shrimps and crabs (Lim & Hudson, 2004; Mi et al., 2001). Attributed to $pK_a < 6.3$, chitosan is soluble in light acidic solvents (i.e., diluted acetic acids) and can be easily modified into different shapes and structures (Ageev, Matushkina, & Vikhoreva, 2007; de Alvarenga, 2011). To date, chitosan has been successfully made into antimicrobial films and scaffolds for medical application, nanofibers, beads and polyelectrolyte complexes (Balmayor, Tuzlakoglu, Marques, Azevedo, & Reis, 2008; Baysal, Aroguz, Adiguzel, & Baysal, 2013; Mi et al., 2001; Sharma, Sanpui, Chattopadhyay, & Ghosh, 2012b). Apart from chitosan, alginate is a polyanionic biopolymer extracted

from seaweed (Bayer, Herrero, & Peppas, 2011; Sharma et al., 2012b). Alginate (β -*D*-mannuronic acids and α -*L*-guluronic acids) has been widely reported for its adsorption capacity towards dyes and heavy metals (Mehta & Gaur, 2005). However, the solubility of alginate in water due to its hydrophilic nature causes alginate to be chemically unstable under aqueous conditions (Young Moon, Pal, & Huang, 1999).

In order to reduce the solubility of alginate, the incorporation of polyanionic alginate with polycationic chitosan forms a stable and insoluble polyelectrolyte complex (PEC) (Sharma et al., 2012b; Young Moon et al., 1999). The use of biopolymer-based membranes can help to overcome the shortcoming of non-biodegradability of conventional membranes and thus, reduce environmental impacts and promote environmental sustainability. However, the application of biopolymers such as chitosan in water filtration is often hindered by its dense structure and mechanical weakness (Ghaee, Shariaty-Niassar, Barzin, & Ismail, 2013). To date, the characteristics of these biopolymers as membrane filtering media and their abilities in the removal of pollutants from wastewater were not thoroughly investigated. Owing to the simplicity in operat-

* Corresponding author at: Chemical Engineering Discipline, School of Engineering, Monash University Malaysia Campus, Jalan Lagoon Selatan, 47500 Bandar Sunway, Selangor, Malaysia.

E-mail address: poh.phaik.eong@monash.edu (P.E. Poh).

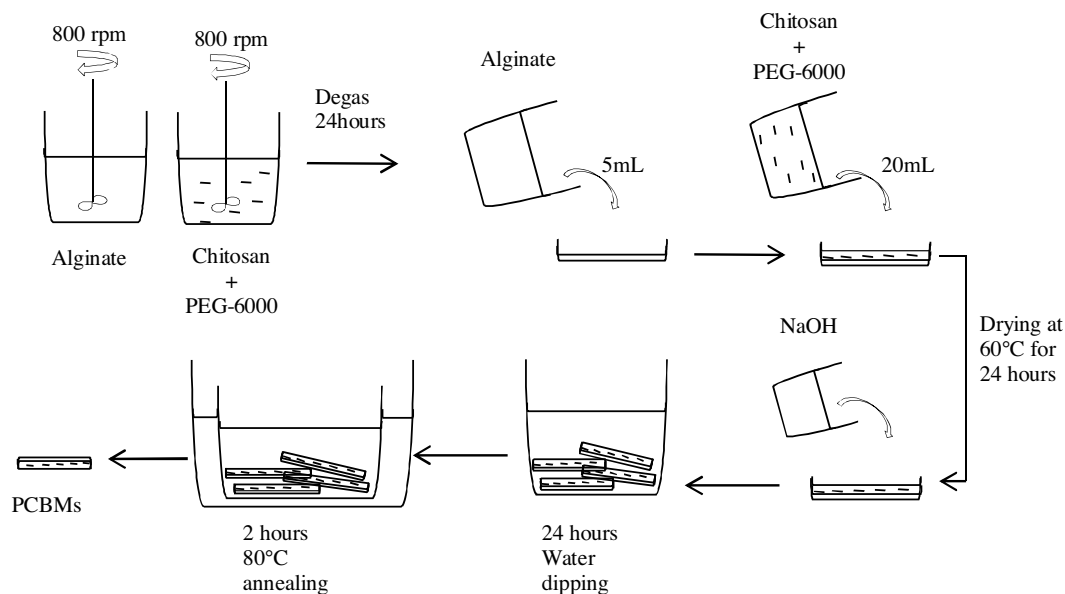


Fig. 1. Flow diagram of PCBM fabrication.

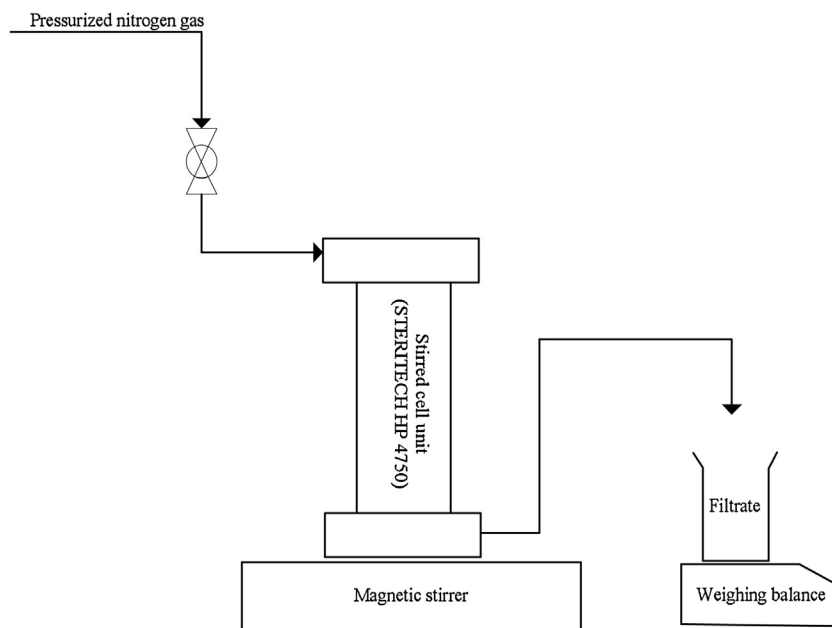


Fig. 2. Stirred cell filtration unit (Sterlitech, HP 4750).

ing membrane filtration systems, they have mostly been used in decentralized greywater systems to remove solids and bacteria as compared to other treatment methods (Ramona, Green, Semiat, & Dosoretz, 2004).

Greywater recycling is gaining impetus as a sustainable urban water solution through direct potable or non-potable augmentation schemes (Ghaitidak & Yadav, 2013; Paulo, Azevedo, Begosso, Galbiati, & Boncz, 2013; Teh, Poh, Gouwanda, & Chong, 2015). Proper and adequate treatment of greywater as a source is essential to minimize the potential public health risks that exist when in physical body contact or through incidental exposures (Alfiya, Gross, Sklarz, & Friedler, 2013; Chong, Cho, Poh, & Jin, 2015; Oh et al., 2015).

Previous studies have shown that the permeation of water fluxes through the membrane used can be improved by incorporating a thin hydrophilic layer on the membrane or blending

hydrophilic materials in the membrane skeletal network (Kumar, Isloor, Ismail, Rashid, & Matsuura, 2013; Young Moon et al., 1999). Thus, the main aim of this study was to incorporate a thin layer of hydrophilic alginate on top of a porous chitosan membrane to form a polyelectrolyte-complex bilayer membrane (PCBM) for application in greywater treatment. The concentration of alginate on the PCBM was varied systematically. In addition, the changes in membrane characteristics and filtration efficiency were investigated due to the formation of PCBM. Finally, the qualities of the treated greywater effluents were compared against the household reclaimed water standard in Canada and Australia (Chaillou, Gérente, Andrès, & Wolbert, 2011; Couto, Calijuri, Assemany, Santiago, & Lopes, 2015). It is anticipated that the PCBM could present a feasible and sustainable water treatment solution for greywater recycling and reuse schemes.

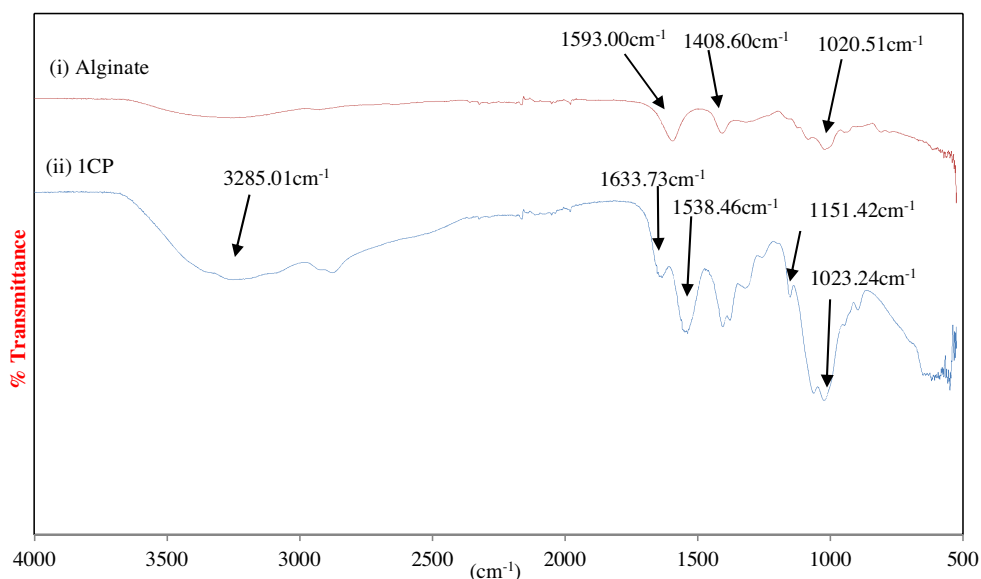


Fig. 3. FTIR spectra of alginate and 1CP membranes.

2. Materials and methods

2.1. Fabrication of PCBM

Specifically, 1 wt% of polyethylene glycol (PEG) was dissolved in 2 vol% of acetic acid to fabricate PCBM. This was followed by the addition of 1 wt% of chitosan into the earlier solvent mixture and continuously stirred for 4 h until a homogenous light yellow solution was obtained. The weight ratio of chitosan: PEG was maintained at 1:1 to produce permeates of consistent quality (Oh, Poh, & Chong, Unpublished work). On the other hand, 0.5 wt% of alginate was dissolved in ultrapure (UP) water. Polymer solutions with 1 wt% and 2 wt% alginate were also prepared. All the homogeneous-stirred solutions were allowed to degas for 24 h to obtain bubble-free solution prior to the membrane casting process.

During the membrane casting process, 5 mL of 0.5 wt% alginate solution was cast on a standard petri dish. Upon successive formation of the alginate membrane layer, 20 mL of chitosan/PEG solution was cast on top of the first alginate layer to form PCBM. PCBMs were also fabricated with 1 wt% and 2 wt% alginate as the first PBCM layer. The cast solution in standard petri dish was placed on a flat surface for approximately 10 min before drying in a convective oven operated at 60 °C for 24 h.

After the convective drying process, the PCBMs were removed from the oven and treated with 2 wt% of sodium hydroxide (NaOH) solution for 15 min. All PCBMs were washed several times with UP water to remove excess NaOH and solvents. The membranes were then removed from the petri dishes and immersed in UP water for 24 h, followed by 2 h immersion in a hot water bath at 80 °C, in order to wash away the PEG in the membrane skeletal network and to generate porous structure. Fig. 1 shows the flow diagram of the fabrication steps and Table 1 gives the PCBM fabrication conditions together with their abbreviations used throughout this study.

Table 1
Membrane fabrication conditions.

Alginate (wt%)	Chitosan:PEG (wt%:wt%)	Membrane name
0	1:1	1CP
0.5	1:1	0.5A1CP
1	1:1	1A1CP
2	1:1	2A1CP

2.2. Membrane characterizations

2.2.1. Physical properties

Fourier transform infrared spectroscopy (FTIR) (Nicolet iS10, Thermo Scientific) was used to identify the molecular structure changes due to the formation of PCBM. Computer software, OMNIC was used to record the infrared spectra of the samples in the range of 525 cm⁻¹ to 4000 cm⁻¹. The spectra were obtained by overlapping 16 scans per run.

Goniometer (Ramé-Hart Instrument Co.) was used to investigate the surface wettability of the PCBMs. In order to study the surface wettability, 0.2 μL of UP water was dropped on the effective surface (i.e., alginate layer). Owing to the changes in contact angle over time, the contact angle was measured at a 6 min interval after water was dropped on the surface.

Scanning electron microscopy (SEM) (Hitachi, S-3400N) was used to observe the morphology of the PCBMs.

Texture analyzer (TA.XT Plus) was used to evaluate the mechanical property of PCBMs. PCBMs were cut into 25 mm × 75 mm films and crosshead speed of 30 mm/min was used to pull the films to their breaking point. The test was repeated five times to obtain average stress and strain of the material.

2.2.2. Swelling equilibrium

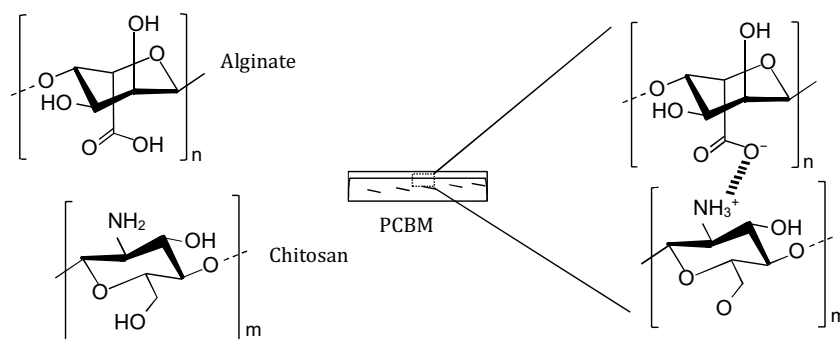
The study of swelling equilibrium was used to investigate the water uptake ability as well as the swelling ability of the 1CP and PCBMs. In order to perform the study, the membranes were cut into small segments (i.e., 1 cm width × 1 cm length) and immersed into UP water at room temperature. Thereafter, the membranes were removed from the UP water bath and wiped with filter paper to remove excess water on the membrane surface. Subsequently, the membranes were weighed at different time intervals of 5, 10, 15, 20, 25, 30, 60, 90 and 120 min. The swelling ratio was calculated using Eq. (1) as shown below:

$$\text{Swelling ratio(\%)} = (W_{\text{wet}} - W_{\text{dry}}) / W_{\text{dry}} \times 100 \quad (1)$$

where W_{wet} is the weight of wet membrane and W_{dry} is the weight of dry membrane.

2.2.3. Water flux

A dead-end stirred cell filtration unit (Sterlitech, HP 4750) was used to perform studies on membrane water flux under various



Scheme 1. Interaction between alginate, chitosan and formation of PCBM.

operating pressures (i.e., 1–4 bar). Bathroom greywater filtration was also performed using the same setup.

A clean membrane was inserted into the dead-end stirred cell on a metallic support, where the cell was loaded with 250 mL of clean UP water. The weight of permeate collected with respect to various operating pressures was recorded using a weighing balance. The duration of water flux study was fixed at 30 min and a stirring speed of 300 rpm. The complete experimental set up is shown in Fig. 2.

Based on the volume of permeate collected from the filtration unit, the water flux was calculated based on Eq. (2) as listed:

$$\text{Flux, } J (\text{L}/\text{m}^2\text{h}) = \frac{V_{\text{permeate}}}{(A \times t)} \quad (2)$$

where V_{permeate} is the volume of permeate collected in liter; A is the effective area of the membrane in m^2 and t is the duration of the filtration in h.

2.2.4. Molecular weight cut-off (MWCO)

MWCO of a membrane is defined as the lowest molecular weight solute (in Da), in which 90–95% of the solute is rejected by the membrane (Schock, Miquel, & Birkenberger, 1989). In essence, 0.1 g of PEG-2000 (P-2000), PEG-3000 (P-3000), PEG-4000 (P-4000), PEG-6000 (P-6000), PEG-10,000 (P-10,000), PEG-100,000 (P-100,000), PEG-350,000 (P-350,000) were dissolved in UP water separately. Thereafter, 250 mL of PEG solution was filled into the dead end stirred cell unit loaded with fresh membrane. Permeate was then collected under the operating pressure of 3 bar and stirring speed of 300 rpm to avoid concentration polarization and accumulation of solutes on the surface of membranes, which might lead to the blockage of pores. A new membrane was used for every molecular weight tested.

Both the feed and permeate were analyzed with a total organic carbon (TOC) analyzer (O.I. Analytical Aurora Model 1030) to determine the TOC concentration before and after solute rejection. The concentration of PEG was determined in terms of TOC and TOC rejection was calculated using Eq. (3) as shown below:

$$\text{Rejection}(\%) = (C_i - C_f)/C_i \times 100 \quad (3)$$

where C_i is the initial TOC concentration of feed solution in mg/L ; C_f is the final TOC concentration of permeates in mg/L .

2.3. Bathroom greywater filtration performance

Bathroom greywater used in this study was collected on the experimental day itself to minimize the bacterial growth due to overnight storage. In addition, the bathroom greywater was contributed by a single source in order to maintain the consistency of the pollutants in the greywater. The characteristics of bathroom greywater used in this study are tabulated in Table 2.

Table 2

Characteristics of bathroom greywater.

Parameters	Unit	min	max
pH	n.a	6.3	6.73
Turbidity	NTU	70.7	160.3
TSS	mg/L or ppm	101.3	206
COD	mg/L or ppm	251	507.5
BOD ₅	mg/L or ppm	81	270.8
<i>E. coli</i>	cfu/100 mL	2.5×10^4	6.1×10^5
Other coliforms	cfu/100 mL	8.5×10^4	53.2×10^4
Pathogenic bacteria	cfu/100 mL	5×10^4	34.1×10^5

2.3.1. Treatment and disinfection efficiency

TSS, turbidity, chemical oxygen demand (COD) and 5-day biological oxygen demand (BOD₅) were analyzed in accordance with the American Public Health Association (APHA) standard methods (Gehr, Wagner, Veerasubramanian, & Payment, 2003). In addition, spread plate technique was used to enumerate *Escherichia coli*, coliforms and pathogenic bacteria. 0.1 mL of raw greywater or treated greywater effluent was transferred onto a standard petri dish containing nutrient agar (Oxoid, Brilliance *E. coli*, CM-1046). The spread plate samples were incubated at 37 °C for 24 h. Bacterial colonies were then reported in terms of colony forming units per 100 mL (cfu/100 mL). All these parameters were measured both before and after the direct membrane filtration treatment using 1CP and PCBMs.

The rejection efficiencies for COD, BOD₅, turbidity, TSS and bacteria of using 1CP and PCBMs were calculated as per Eq. (4):

$$\text{Rejection}(\%) = (C_{\text{initial}} - C_{\text{final}})/C_{\text{initial}} \times 100 \quad (4)$$

where C_i and C_f are the concentration of pollutants from the inlet and outlet streams, respectively.

3. Results and discussion

3.1. Membrane characterization

3.1.1. Molecular structure

Figs. 3 and 4 show the FTIR spectra for alginate, 1CP membrane and PCBM. As shown in Fig. 3(i), the FTIR peaks at 1020.51 cm^{-1} , 1593.00 cm^{-1} and 1408.60 cm^{-1} indicate the presence of carboxylic acid functional groups, as well as asymmetric and symmetric carboxylate anions of alginate (Sharma, Sanpui, Chattopadhyay, & Ghosh, 2012a). On the other hand, for the 1CP membrane as shown in Fig. 3(ii), the broaden FTIR peak at 3285.01 cm^{-1} indicates the presence of O–H and N–H stretching (i.e., 3000–3500 cm^{-1}), while the FTIR absorption peaks at 1633.73 cm^{-1} and 1538.46 cm^{-1} correspond to amide I (1600–1670 cm^{-1}) and amide II (1550–1640 cm^{-1}), respectively. In addition, 1151.42 cm^{-1} and 1023.24 cm^{-1} are the absorption

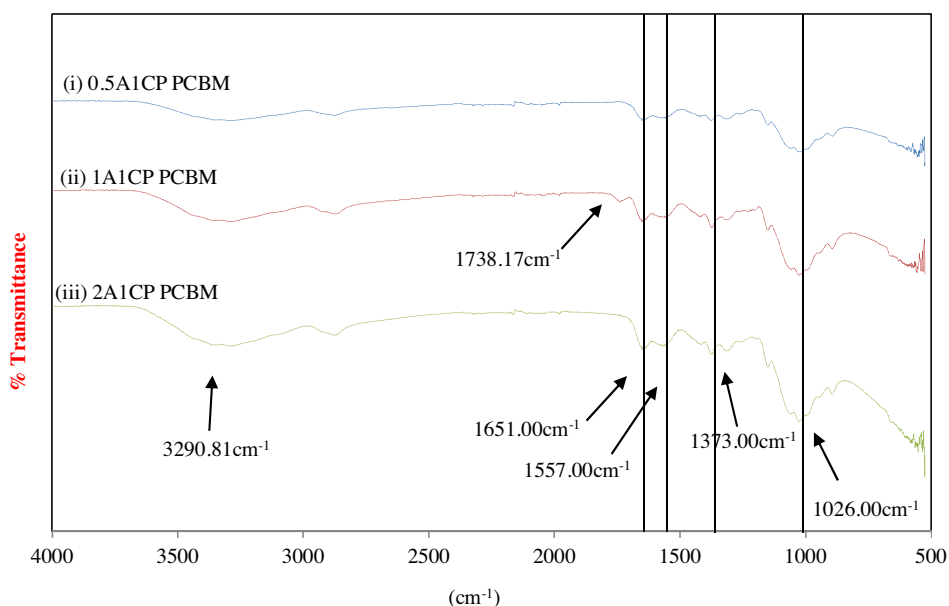


Fig. 4. FTIR spectra of PCBMs.

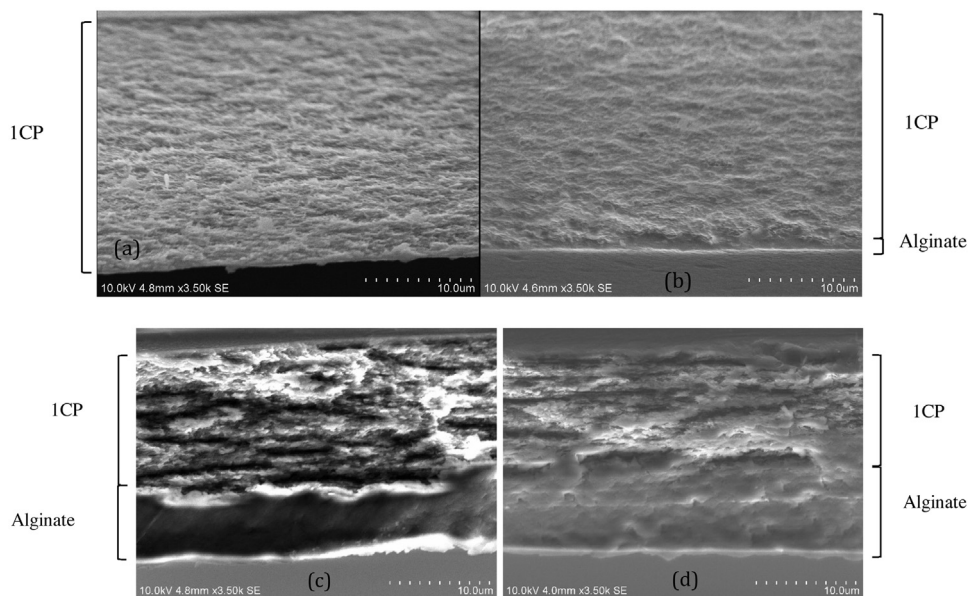


Fig. 5. (a) Cross section of 1CP membrane (b) Cross section of 0.5A1CP membrane (c) Cross section of 1A1CP membrane (d) Cross section of 2A1CP membrane.

bands for the amino group and C–O ($1000\text{--}1300\text{ cm}^{-1}$) in chitosan, respectively.

Due to the small amount of alginate added, the PCBM spectra shown in Fig. 4(i)–(iii) have similar structures as the 1CP membrane, since 1CP forms the main structure of the membrane. The FTIR peaks at 1538.46 cm^{-1} and 1633.73 cm^{-1} originally present in 1CP were shifted to 1557 cm^{-1} to 1651 cm^{-1} after the incorporation of alginate. Scheme 1 shows the interaction between alginate and chitosan during the fabrication of PCBMs. The two broad peaks present for the three FTIR spectra in the range of 1557 cm^{-1} to 1651 cm^{-1} correspond to the overlapping of amide groups of chitosan and carboxyl anions in the alginate (as shown in Scheme 1) (Coates, 2006; Sharma et al., 2012a). Thus, the presence of these two peaks in the FTIR spectra confirmed the interaction between the chitosan and alginate layers. Other than that, when the concentration of alginate increases with fixed chitosan/PEG concentration,

the peak intensity at 1373 cm^{-1} (i.e. N–O bonding) also increases. The increase in the intensity of this peak show the formation of increased N–O bonding due to the interaction between the carboxylic groups in alginate with the amide group in chitosan. In addition, the rise in the intensity of peak 1026 cm^{-1} (i.e., carboxylic acids) and 3290.81 cm^{-1} (i.e., hydroxyl group) with the increase in alginate concentration indicated the presence of alginate in the PCBMs.

3.1.2. Membrane structure

The cross sectional structure of the membranes was studied in order to identify the structural change in the membranes. The cross sectional structure of the 1CP membrane is shown in Fig. 5(a). On the other hand, Fig. 5(b)–(d) display the PCBM structures, where the top layer consists of porous chitosan while the bottom layer consists of alginate layer. The two distinct layers of membranes

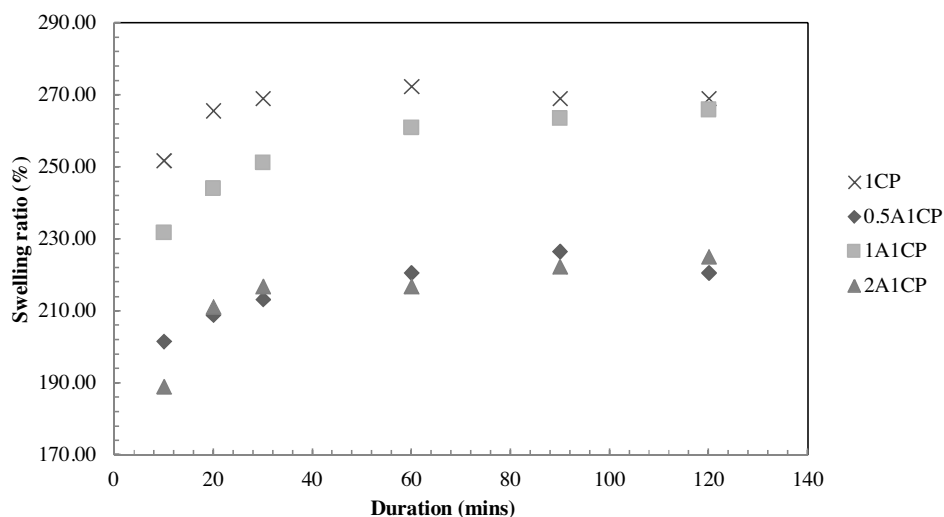


Fig. 6. Swelling curves of 1CP and PCBMs.

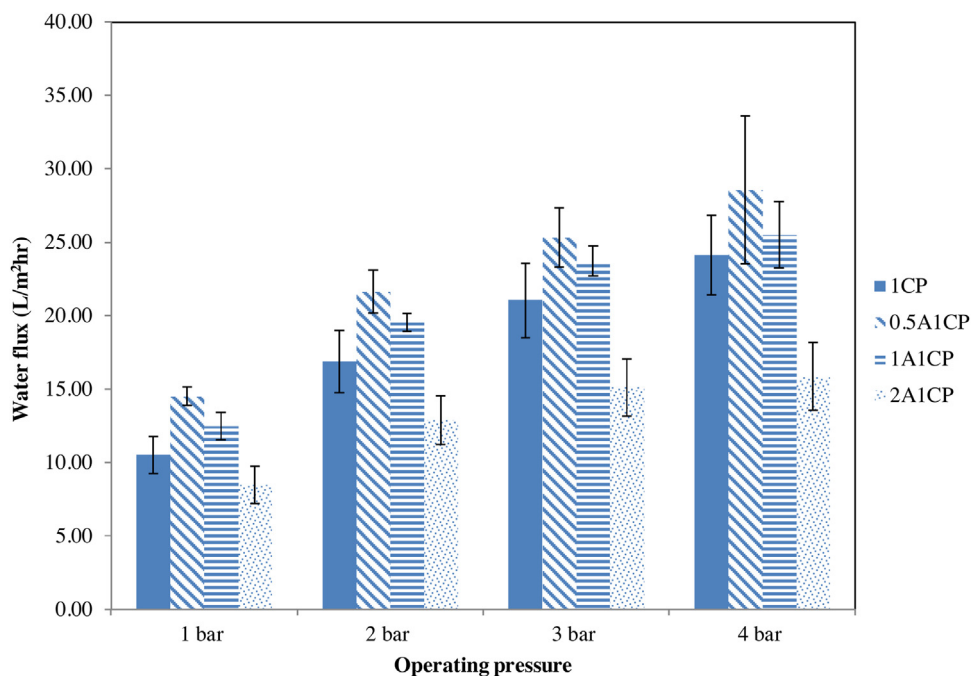


Fig. 7. UP water flux of 1CP and PCBM membranes.

observed confirmed the formation of PCBM. From the images, it can be deduced that the formation of polyelectrolyte complex between alginate and chitosan occurs at the interface of the two layers. As previously discussed in Section 3.1.1, the FTIR peaks shown in 1557 cm^{-1} to 1651 cm^{-1} after the incorporation of alginate verified the interaction between chitosan and alginate biopolymers. The formation of the dense bottom alginate layer was due to the absence of porogen and resulted in strong intermolecular interaction between alginate biopolymer itself. Other than that, it was found that the layer becomes thicker as the concentration of the pure alginate increased from 0.5 wt% up to 2 wt%. The increasing thickness of alginate layer was due to the increase in concentration of alginate polymer in the casting solution.

In addition, the tensile strength of the 1CP membrane was found to be $41.55 \pm 5.32\text{ MPa}$ and strain of $2.248 \pm 0.65\%$. The incorporation of increased alginate concentration in PCBM resulted in higher tensile strength and strain of the membrane. The increase

in alginate concentration from 0.5 wt% to 2 wt%, increased the tensile strength of membranes by a total of 34.2%. The tensile strength of the PCBMs was found to range from $50.37 \pm 8.76\text{ MPa}$ to $63.24 \pm 10.03\text{ MPa}$ and strain of $3.43 \pm 0.99\%$ to $4.16 \pm 0.97\%$ with the increase in alginate concentration. This indicates that incorporation of alginate in 1CP membranes strengthens the structure in addition to the hydrophilicity of the membrane.

3.1.3. Swelling ratio

The swelling ratio is an useful indicator to identify the degree of crosslinking of the membrane (Rhim, 2004). High degree of crosslinking leads to a low water penetration, which results in low swelling in the biopolymer network (Vimala et al., 2010). The swelling curves of PCBMs are recorded in Fig. 6. Generally, it can be observed that PCBMs have a lower swelling capability as compared to 1CP membranes. This is mainly attributed to the formation of polyelectrolyte complexes between the protonated amino groups

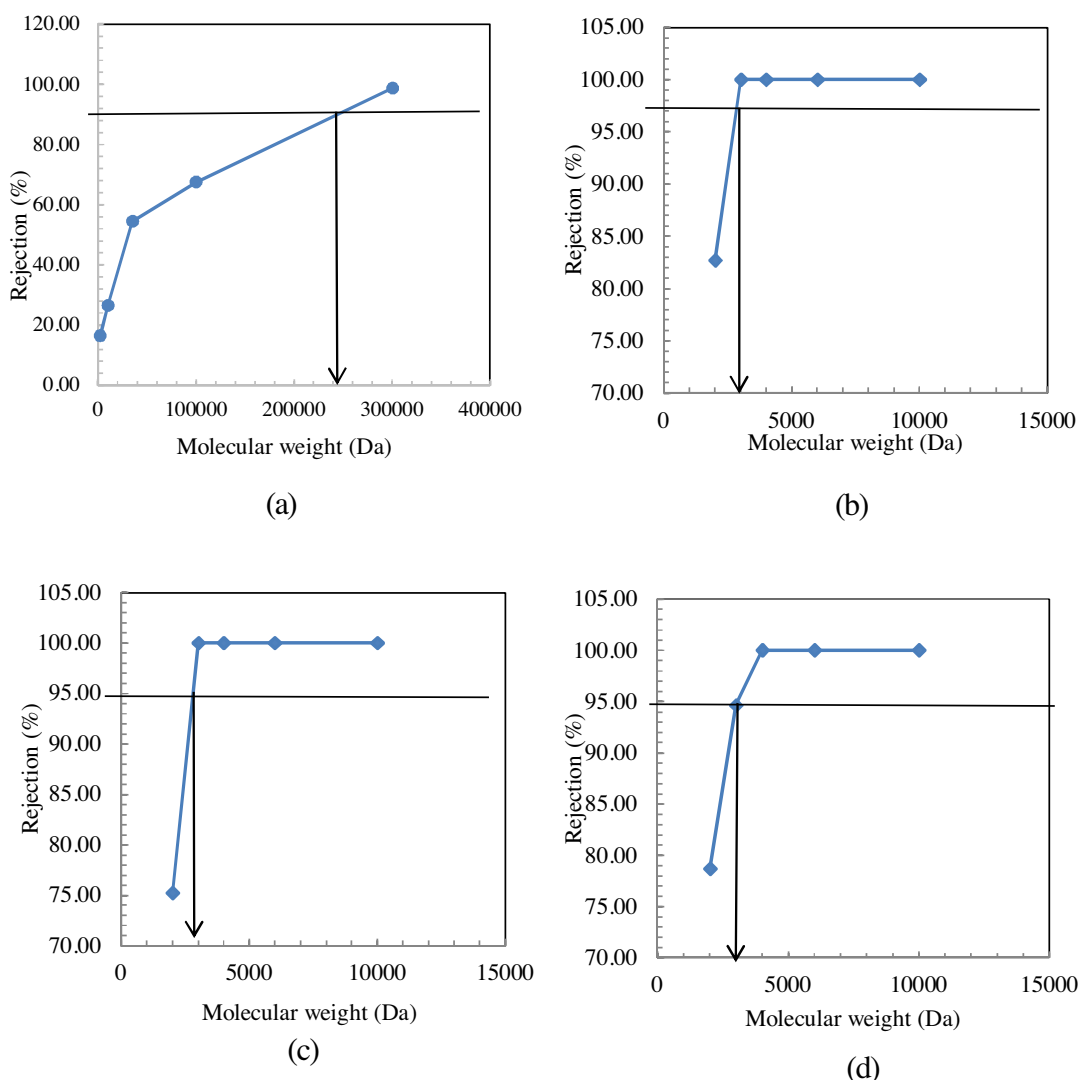


Fig. 8. (a) MWCO of 1CP membrane (b) MWCO of 0.5A1CP PCBM (c) MWCO of 1A1CP PCBM (d) MWCO of 2A1CP PCBM.

and carboxylate groups of alginate (shown in Scheme 1) that cause the reduction in the functional groups responsible for water uptake (Sharma et al., 2012a).

From the swelling curves, it was found that all the PCBMs reached the swelling equilibrium after 60 min. At 60 min, the swelling ratios of 1A1CP and 2A1CP PCBMs are 261.0% and 216.7%, respectively. The swelling ratio of 0.5A1CP is 220.6%. This indicates that the 1A1CP membrane has a lower ionic crosslinking degree and thus, a higher swelling as compared to the 2A1CP membrane. It can be observed from the FTIR spectrum peak of 1A1CP membrane at 1738.17 cm^{-1} (Fig. 4) that there is a significant presence of the carboxylic functional group ($\text{C}=\text{O}$) in alginate. This suggests the strong intermolecular interaction of alginate biopolymer at 1 wt% concentration, which also could be the cause of lower crosslinking degree in the 1A1CP PCBM. As for 0.5A1CP membrane, the low surface tension of alginate at 0.5 wt% alginate concentration, as compared to those at higher alginate concentrations (i.e., 1 wt% and 2 wt%) (Lee, Chan, Ravindra, & Khan, 2012) appears to be more dispersed and could easily interact with chitosan due to the weak intermolecular interaction of alginate. Nevertheless, the swelling ratio of PCBM is lower than 1CP membrane indicating the interaction between alginate and chitosan.

3.1.4. Surface wettability

The alginate surface was selected as the membrane active surface in order to evaluate its surface wettability. This is due to the fact that the addition of alginate layer in PCBM is aimed to improve both the membrane rejection efficiency and surface wettability via the formation of hydrophilic alginate layer on chitosan membrane.

Before alginate was complexed with chitosan to form PCBM, the contact angle of the 1CP membrane was measured at $88.10^\circ \pm 1.02^\circ$. Initially, the contact angle of PCBM declined when 0.5 wt% of alginate was introduced, and then increased when the concentration of alginate was increased from 1 wt% to 2 wt%. The surface contact angle was found to be $67.51 \pm 0.01^\circ$ for 0.5 wt%, $79.66 \pm 1.18^\circ$ for 1 wt% and $87.49^\circ \pm 0.45^\circ$ for 2 wt% alginate as shown in Table 3. The higher surface water contact angle measured in 1CP membrane is mainly attributed to the porous structure in the membrane net-

Table 3
Surface water contact angle ($^\circ$) of various fabricated PCBMs.

Membrane	Surface contact angle ($^\circ$)
1CP	88.10 ± 1.02
0.5A1CP	67.51 ± 0.01
1A1CP	79.66 ± 1.18
2A1CP	87.49 ± 0.45

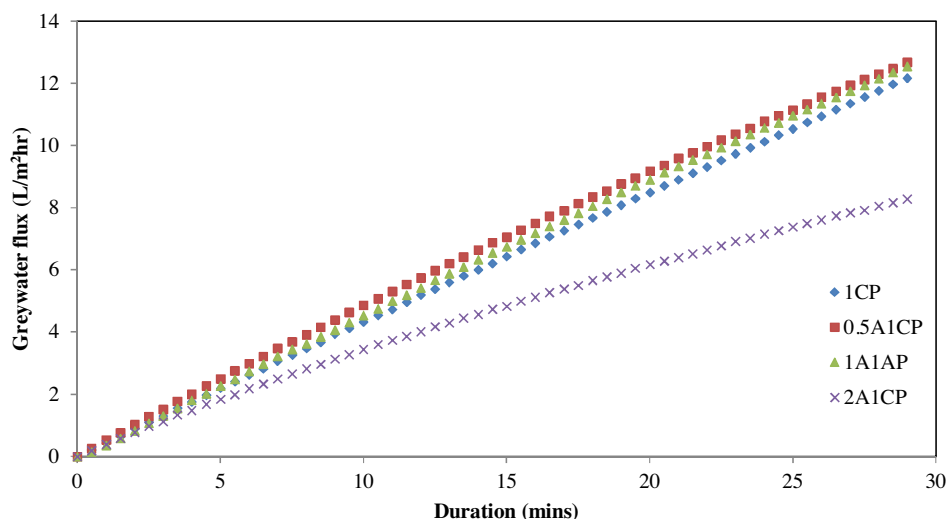


Fig. 9. Greywater flux of various membranes.

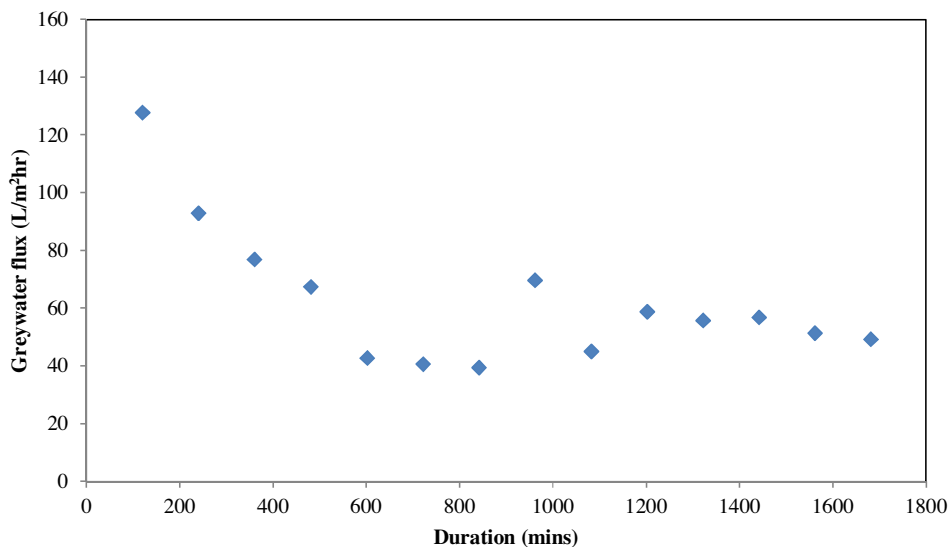


Fig. 10. Greywater filtration flux of 15 cycles using 0.5A1CP PCBM (2 h per cycle).

work. The presence of an air gap under the water droplet resulted in higher water contact angle (Yuan & Lee, 2013) as compared to other PCBMs. As the dense alginate layer formed on top of the porous 1CP membrane, the hydrophilicity of alginate hindered the effect of the air gap on the water droplets and thus, resulted in the decrease in water contact angle of PCBMs.

Form the observed trend in surface contact angle, it can be deduced that the presence of alginate for complexation with chitosan is the main contributor that dictates such changes in PCBM. Lee et al., (2012) also reported an increase in surface tension of biopolymer solution with increasing alginate concentration from 0.5 wt% to 2 wt% (Lee et al., 2012). This indicates that at low alginate concentration, the weak surface tension (or surface energy) of alginate polymers results in a stronger intermolecular interaction between alginate and water molecules. Therefore, the alginate surface can be easily wet at low alginate concentration. As the concentration of alginate increases, the surface tension (or surface energy) of alginate also increases, resulting in strong intermolecular interaction between alginate polymer chains. This causes difficulty for water to wet the surface of the membrane, hence resulting in higher water contact angle.

Incorporation of alginate, especially with low concentration alginate, has led to a better membrane surface wettability as compared to the 1CP membrane. However, the surface wettability reduced when higher concentration of alginate was loaded and resulted in the reduction of permeate water fluxes. Thus, the latter part of the study involved the investigation of membrane permeate water fluxes under various operating pressures after the alginate loadings.

3.1.5. UP water flux

In order to investigate the effect of alginate-complexed layer on permeate water flux, the UP water fluxes of PCBMs were tested under various pressure conditions (Fig. 7). Due to the fact that the PCBM is mainly targeted for application in decentralized greywater treatment, the treatment system was not operated at very high operating pressure as a safety precaution and energy minimization effort. Therefore, the maximum operating pressure investigated in this study was 4 bar.

Through this study, the permeate water flux was found to be the lowest at an operating pressure of 1 bar with an increasing trend against the operating pressure. The average UP water flux for

the 1CP membrane ranged from 10.52 L/m²h to 24.06 L/m²h when the operating pressure was varied from 1 to 4 bar. The 0.5A1CP PCBMs showed the highest range of water flux readings with values between 14.51 L/m²h and 28.57 L/m²h under similar operating pressure conditions. However, the UP water flux produced by 1A1CP and 2A1CP PCBMs showed a declining trend as compared to the 0.5A1CP and 1CP membranes. The water fluxes produced by PCBMs were very much dependent on the concentration of alginate and surface wettability. Other than that, based on the cross section images of the membranes in Fig. 5(a)–(d), it is observed that the increase in alginate concentration results in an increased thickness on the alginate layer, leading to a higher resistance of water molecules permeating through the membranes. In addition, as discussed in Section 3.1.4, the increase in alginate concentration was found to enhance the hydrophobicity of membranes, causing the PCBMs with higher alginate concentration to experience low permeation of UP water. Thus, the concentration of alginate in PCBMs should be minimized to avoid excessive flux reduction. Alternatively, porogens can also be introduced in alginate to enhance the porosity and thus improve the overall water flux.

3.1.6. Molecular weight cut-off (MWCO)

In this study, MWCO is used to determine the minimum size of solute that can be removed by the fabricated PCBMs. Prior to the complexation of alginate with chitosan to form PCBMs, the MWCO of pure chitosan 1CP membrane was found to be approximately 242 kDa (Fig. 8(a)). The complexation of alginate with chitosan to form PCBMs is expected to lower the pore sizes or MWCO due to the higher degree of crosslinking (Zeng & Fang, 2004). From Fig. 8(b)–(d), it was found that the MWCO of PCBMs was down shifted from 242 kDa (1CP) to the range of 2.71 kDa–3.08 kDa. The MWCO of PCBMs with increasing amount of alginate did not vary drastically. The MWCO of PCBMs falls in the narrow margin mainly due to the fact that the formation of PEC occurs at the interface of alginate and chitosan, but not throughout the entire biopolymer network. Thus, this has only resulted in a 12% difference in the MWCO values of these membranes. Nevertheless, the incorporation of alginate layer on the 1CP membrane significantly reduced the MWCO. With the low MWCO in PCBMs, the membrane could remove greater amounts of pollutants from greywater than the 1CP membrane. All the membranes were tested in greywater filtration to understand the effect of incorporation of alginate in removing the pollutants.

3.2. Greywater treatment

From the previous section, it was shown that the optimum MWCO of PCBMs ranged between 2.71 kDa and 3.08 kDa. Thus, the following studies aim is to verify the ability of PCBMs in the removal of pollutants from greywater.

3.2.1. Treatment performance

In general, PCBMs show superior ability in the removal of TSS and turbidity. In essence, 99.9% removal of turbidity and 100% removal of TSS were achieved using PCBMs. In addition, PCBMs showed higher turbidity removal efficiency of 5.2% higher than the 1CP membrane. PCBMs managed to produce treated greywater effluents that meet the non-potable reuse standard of <5 NTU for turbidity and <30 mg/L for TSS.

Furthermore, it was observed that the reduction of membrane MWCO actually contributes to an improved removal of fine organic pollutants (i.e., COD) when compared to the 1CP membrane. As tabulated in Table 4, only 60.9% COD was removed using the 1CP membrane, while COD removal with PCBMs was found to range from 80.8% to 85.5%. This implies that a 19.9% to 24.6% improvement in terms of COD removal can be achieved through the use of PCBMs

Table 4
Greywater treatment efficiency using PCBMs.

Parameters	Unit	1CP	0.5A1CP	1A1CP	2A1CP
pH	n.a	6.65	6.84	6.94	6.99
Turbidity	%	94.7	99.9	99.9	99.9
TSS	%	100.0	100.0	100.0	100.0
COD	%	60.9	83.2	80.8	85.5
BOD ₅	%	61.5	53.7	59.7	86.6
<i>E. coli</i>	%	n.a	100.0	100.0	99.9
Other coliforms	%	n.a	100.0	99.8	100.0
Pathogenic bacteria	%	100.0	99.7	81.6	99.0

for greywater filtration. As reported by Hocaoglu, Atasoy, Baban, and Orhon (2013), most of the COD size distribution is in the size range of >1.2 μm and 14 nm to 220 nm. Thus, it can be deduced that the reduction in MWCO has resulted in higher removal efficiency of finer-sized COD (i.e., 14 nm to 220 nm).

Additionally, it is observed that the BOD₅ removal efficiency of PCBMs is enhanced when the concentration of the alginate layer increases. The increasing amount of anionic alginate biopolymer at higher alginate concentrations would also result in higher repulsion of Gram-negative microorganisms. Therefore, the BOD₅ removal efficiency was found to be higher when the concentration of alginate increased. The BOD₅ removal efficiencies of using PCBMs were found to be 53.7–86.6%. The relatively lower BOD₅ removal efficiencies of 0.5A1CP and 1A1CP membranes could be attributed to the thinner alginate layer that allows a higher amount of microorganism to penetrate through the membrane.

Greywater disinfection was carried out to investigate the ability of PCBMs in removing bacteria from the greywater. Overall, the PCBMs showed 99.9–100% removal of *E. coli*, 99.8–100% removal of other coliforms and 81.6–99.7% removal of pathogenic bacteria. Despite the reduction in bacteria, the treated greywater effluents produced using PCBMs did not meet the reuse standard in terms of pathogenic bacteria. Bacteria were found to escape from the membrane filtration system even though there was a down shift in the MWCO of PCBMs. Guo and Santschi (2007) presented an example of 0.02 μm (300 kDa) membrane having the actual MWCO of 3 kDa, which was due to the difference in the structure or shape of the filtering particles. This indicated that the contaminant removal efficiency might vary as the shape and the structure of the contaminants differ in the raw greywater and resulted in the escaped of pollutants through the membrane. In addition, attributed to the formation of PEC between chitosan and alginate biopolymers and pH of greywater from 6.65 to 6.99, the antimicrobial property of chitosan could be reduced due to lack of interactions between positive functional groups of chitosan with the bacteria.

Greywater flux of various membranes was recorded for the duration of 30 min (Fig. 9). Higher greywater flux was recorded for 0.5A1CP and 1A1CP PCBMs compared to 1CP, whilst 2A1CP had the lowest greywater flux. The study coincides with the finding of UP water flux in Section 3.1.5, where 0.5A1CP PCBMs has highest water flux. Hence, 0.5A1CP PCBMs was selected to further evaluate the greywater flux for 15 cycles of 2 h filtration per cycle. The fresh membrane was found to have highest greywater flux (127.99 L/m²h), as the pores of the fresh membrane were not clogged up by the pollutants in the greywater. Greywater flux declined on the second and third cycle due to the accumulation of pollutants on the surface of the membrane. As shown in Fig. 10, after the fourth cycle of greywater filtration, 0.5A1CP PCBMs started to produce treated greywater with consistent greywater flux.

Overall, it was found that PCBMs have better removal efficiency in terms of TSS and turbidity removal as compared to the 1CP membrane. It also showed that the COD and BOD₅ removal increases with the increase in alginate concentration. However, trace amounts of bacteria were found in the treated greywater

effluent, which suggests further improvements are required on the membrane and the system. For instance, the incorporation of biocides in the membrane network or the coupling of the membrane system with an additional disinfection unit such as, UV treatment, chlorine or ozone dosage would help further disinfect the treated greywater prior delivering to the end users.

4. Conclusion

In conclusion, the complexation of alginate with chitosan to form PCBMs was successfully fabricated for greywater filtration treatment. Hydrophilic alginate was added and complexed on top of porous chitosan membrane to form PCBMs, with the aim to improve water permeation flux and pollutant removal efficiency. The formation of a thick alginate layer resisted the passage of water molecules and reduced water flux. Thus, the concentration of the hydrophilic alginate layer has to be minimized in order to avoid the formation of a thick, dense, alginate layer or further modifications could be done to generate porous network within the hydrophilic layer. In addition, the incorporation of alginate down shifted the MWCO of 242 kDa for the 1CP membrane to values ranging between 2.71 kDa and 3.08 kDa for PCBMs. The reduction in MWCO of the membranes improved the treatment efficiency of PCBMs as compared to pure chitosan 1CP membrane. Greywater treatment using 0.5A1CP membrane, could remove of 99.9% of turbidity, 100% of TSS, 83.2% of COD, 53.7% of BOD₅, 100% of *E. coli*, 100% other coliforms and 99.7% of pathogenic bacteria.

Acknowledgement

The author would like to acknowledge Monash University Malaysia for the financial support to this project.

References

- Ageev, E., Matushkina, N., & Vikhoreva, G. (2007). Pervaporation properties of thermally modified chitosan films. *Colloid Journal*, 69(3), 272–277.
- Alfiya, Y., Gross, A., Sklarz, M., & Friedler, E. (2013). Reliability of on-site greywater treatment systems in Mediterranean and arid environments—a case study. *Water Science & Technology*, 67(6), 1389–1395.
- Balmayor, E. R., Tuzlakoglu, K., Marques, A. P., Azevedo, H. S., & Reis, R. L. (2008). A novel enzymatically-mediated drug delivery carrier for bone tissue engineering applications: combining biodegradable starch-based microparticles and differentiation agents. *Journal of Materials Science: Materials in Medicine*, 19(4), 1617–1623.
- Bayer, C. L., Herrero, É. P., & Peppas, N. A. (2011). Alginate films as macromolecular imprinted matrices. *Journal of Biomaterials Science, Polymer Edition*, 22(11), 1523–1534.
- Baysal, K., Aroguz, A. Z., Adiguzel, Z., & Baysal, B. M. (2013). Chitosan/alginate crosslinked hydrogels: preparation: characterization and application for cell growth purposes. *International Journal of Biological Macromolecules*, 59, 342–348.
- Chaillou, K., Gérente, C., Andrès, Y., & Wolbert, D. (2011). Bathroom greywater characterization and potential treatments for reuse. *Water, Air, & Soil Pollution*, 215(1–4), 31–42.
- Chong, M. N., Cho, Y. J., Poh, P. E., & Jin, B. (2015). Evaluation of titanium dioxide photocatalytic technology for the treatment of reactive Black 5 dye in synthetic and real greywater effluents. *Journal of Cleaner Production*, 89, 196–202.
- Coates, J. (2006). Interpretation of Infrared Spectra. A Practical Approach. In *Encyclopedia of Analytical Chemistry*. John Wiley & Sons, Ltd., pp. 1–23.
- Couto, E. d. A. d., Calijuri, M. L., Assemany, P. P., Santiago, A. d. F., & Lopes, L. S. (2015). Greywater treatment in airports using anaerobic filter followed by UV disinfection: an efficient and low cost alternative. *Journal of Cleaner Production*, 106, 372–379.
- de Alvarenga, E. S. (2011). Characterization and properties of chitosan. *Biotechnology of Biopolymers*, 91.
- Gehr, R., Wagner, M., Veerasubramanian, P., & Payment, P. (2003). Disinfection efficiency of peracetic acid, UV and ozone after enhanced primary treatment of municipal wastewater. *Water Research*, 37(19), 4573–4586.
- Ghaee, A., Shariaty-Niassar, M., Barzin, J., & Ismail, A. (2013). Chitosan/polyethersulfone composite nanofiltration membrane for industrial wastewater treatment. *International Journal of Nanoscience and Nanotechnology*, 9(4), 213–220.
- Ghaidak, D., & Yadav, K. (2013). Characteristics and treatment of greywater—a review. *Environmental Science and Pollution Research*, 20(5), 2795–2809.
- Guo, L., & Santschi, P. H. (2007). Ultrafiltration and its applications to sampling and characterisation of aquatic colloids. *IUPAC Series on Analytical and Physical Chemistry of Environmental Systems*, 10, 159.
- Hocaoğlu, S. M., Atasoy, E., Baban, A., & Orhon, D. (2013). Modeling biodegradation characteristics of grey water in membrane bioreactor. *Journal of Membrane Science*, 429, 139–146.
- Kumar, R., Isloor, A. M., Ismail, A. F., Rashid, S. A., & Matsuura, T. (2013). Polysulfone–Chitosan blend ultrafiltration membranes: preparation, characterization, permeation and antifouling properties. *Rsc Advances*, 3(21), 7855–7861.
- Lee, B.-B., Chan, E.-S., Ravindra, P., & Khan, T. A. (2012). Surface tension of viscous biopolymer solutions measured using the du Nouy ring method and the drop weight methods. *Polymer Bulletin*, 69(4), 471–489.
- Lim, S.-H., & Hudson, S. M. (2004). Synthesis and antimicrobial activity of a water-soluble chitosan derivative with a fiber-reactive group. *Carbohydrate Research*, 339(2), 313–319.
- Mehta, S., & Gaur, J. (2005). Use of algae for removing heavy metal ions from wastewater: progress and prospects. *Critical Reviews in Biotechnology*, 25(3), 113–152.
- Mi, F.-L., Shyu, S.-S., Wu, Y.-B., Lee, S.-T., Shyong, J.-Y., & Huang, R.-N. (2001). Fabrication and characterization of a sponge-like asymmetric chitosan membrane as a wound dressing. *Biomaterials*, 22(2), 165–173.
- Oh, K. S., Poh, P. E., Chong, M. N., Gouwanda, D., Lam, W. H., & Chee, C. Y. (2015). Optimizing the in-line ozone injection and delivery strategy in a multistage pilot-scale greywater treatment system: System validation and cost-benefit analysis. *Journal of Environmental Chemical Engineering*, 3(2), 1146–1151.
- Oh K. S., Poh P. E., & Chong M. N. (Unpublished work). Greywater treatment using chitosan membrane: understanding the effects of Polyethylene Glycol (PEG) on physicochemical properties and greywater filtration efficiency.
- Paulo, P. L., Azevedo, C., Begosso, L., Galbiati, A. F., & Boncz, M. A. (2013). Natural systems treating greywater and blackwater on-site: integrating treatment, reuse and landscaping. *Ecological Engineering*, 50, 95–100.
- Ramona, G., Green, M., Semiat, R., & Dosoretz, C. (2004). Low strength graywater characterization and treatment by direct membrane filtration. *Desalination*, 170(3), 241–250.
- Rhim, J.-W. (2004). Physical and mechanical properties of water resistant sodium alginate films. *LWT—Food Science and Technology*, 37(3), 323–330.
- Schock, G., Miquel, A., & Birkenberger, R. (1989). Characterization of ultrafiltration membranes: cut-off determination by gel permeation chromatography. *Journal of Membrane Science*, 41, 55–67.
- Sharma, S., Sanpui, P., Chattopadhyay, A., & Ghosh, S. S. (2012a). Fabrication of antibacterial silver nanoparticle–sodium alginate–chitosan composite films. *RSC Advances*, 2(13), 5837–5843.
- Sharma, S., Sanpui, P., Chattopadhyay, A., & Ghosh, S. S. (2012b). Fabrication of antibacterial silver nanoparticle–sodium alginate–chitosan composite films. *RSC Advances*, 2(13), 5837–5843.
- Teh, X. Y., Poh, P. E., Gouwanda, D., & Chong, M. N. (2015). Decentralized light greywater treatment using aerobic digestion and hydrogen peroxide disinfection for non-potable reuse. *Journal of Cleaner Production*, 99, 305–311.
- Vimala, K., Mohan, Y. M., Sivudu, K., Varaprasad, K., Ravindra, S., Reddy, N. N., et al. (2010). Fabrication of porous chitosan films impregnated with silver nanoparticles: a facile approach for superior antibacterial application. *Colloids and Surfaces B: Biointerfaces*, 76(1), 248–258.
- Young Moon, G., Pal, R., & Huang, R. Y. M. (1999). Novel two-ply composite membranes of chitosan and sodium alginate for the pervaporation dehydration of isopropanol and ethanol. *Journal of Membrane Science*, 156(1), 17–27.
- Yuan, Y., & Lee, T. R. (2013). Contact angle and wetting properties. In *Surface science techniques*. pp. 3–34. Springer.
- Zeng, M., & Fang, Z. (2004). Preparation of sub-micrometer porous membrane from chitosan/polyethylene glycol semi-IPN. *Journal of Membrane Science*, 245(1–2), 95–102.